Nat. Hazards Earth Syst. Sci. Discuss., 2, 4813–4830, 2014
www.nat-hazards-earth-syst-sci-discuss.net/2/4813/2014/
doi:10.5194/nhessd-2-4813-2014

Natural Hazards and Earth System Sciences
Open Access
Discussions

Process-related deformation monitoring by PSI using high resolution space-based SAR data: a case study in Düsseldorf, Germany

D. Liu[1], A. Sowter[2], and W. Niemeier[1]

[1]Institute of Geodesy and Photogrammetry, TU Braunschweig, Braunschweig, Germany
[2]Nottingham Geospatial Institute, University of Nottingham, Nottingham, UK

Received: 9 July 2014 – Accepted: 15 July 2014 – Published: 31 July 2014

Correspondence to: D. Liu (donglie.liu@tu-bs.de)

Published by Copernicus Publications on behalf of the European Geosciences Union.

Abstract

TerraSAR-X satellite SAR (Synthetic Aperture Radar) scenes have been analysed using Persistent Scatter Interferometry (PSI) approach to monitor a tunnelling process in Düsseldorf, Germany. The aim of this work is to detect the deformation of ground surface and structures above the tunnelling line during the tunnel excavation. In this study, the PSI approach integrated in the open source software package Stanford Method for Persistent Scatterers (StaMPS) was employed since it has shown significant advantages in obtaining Persistent Scatterers (PS). In order to protect the historic buildings in this region from subsidence-induced damages, a Tunnel Boring Machine (TBM) was used to restrain serious displacements during the tunnelling excavation, as well as compensation injections. Both surface uplifting and subsidence were observed during this tunnelling process, by a levelling survey and a validated PSI observation. It is concluded that sub-centimetre accuracy observations are achievable for process-related monitoring in urban areas, using the open source software package.

1 Introduction

Ground subsidence has strong impacts not only on local structure stability, but also on regional topographic changes. The excavation of underground systems is a typical cause of subsidence in both urban and non-urban areas (Lu and Danskin, 2001; Catalao et al., 2011; Liu et al., 2014). For instance, land subsidence is frequently caused by subway construction in cities all over the world. Nevertheless, urban tunnelling requires that the ground surface should be undisturbed. Therefore, a Tunnel Boring Machine (TBM) is routinely used for excavation due to its low disturbance of the surrounding ground, although the upfront cost is expensive (Schindler et al., 2014). Apart from TBM, compensation injections may also be applied along the tunnelling line (Mark et al., 2012).

NHESSD
2, 4813–4830, 2014

Interferometric Synthetic Aperture Radar (InSAR) and Persistent Scatterers Interferometry (PSI) produce a time series of deformation on a succession of time-ordered images, in principle allowing people to investigate temporal characteristics of deformation patterns (Massonnet et al., 1993; Bamler and Hartl, 1998; Osmanoğlu et al., 2011; Liu et al., 2014). Several InSAR/PSI techniques have been developed for deformation monitoring in the past years (Berardino et al., 2002; Lanari et al., 2004; Hooper et al., 2007; Pritchard and Fielding, 2008; Sowter, 2010; Li et al., 2011; Crosetto et al., 2013; Sowter et al., 2013). In contrast to other PSI method, Stanford Method for Persistent Scatterers (StaMPS) has shown its strong abilities for monitoring non-urban areas (Hooper, 2006). However exciting these developments people have made, there are still challenges when applying PSI to monitor subtle deformation by removing signal contamination from, i.e. atmosphere and DEM errors.

In this paper, we have applied StaMPS to monitor a tunnelling process for a subway construct in Düsseldorf, Germany. Using 20 high resolution TerraSAR-X images, a time series of surface displacement at the control point induced by tunnel excavation has been extracted with millimetre-level accuracy, validated by a levelling survey.

2 Methodology

Starting from single-look complex (SLC) images, 20 scenes of TerraSAR-X data are imported directly into the Delft Object-oriented Radar Interferometric Software (DORIS) and used to form interferograms (Kampes and Usai, 1999). We select the master scene that minimizes the sum de-correlation of all interferograms, while the temporal baselines, spatial baselines, Doppler centroid baselines and thermal noise are also considered. The 90 m Shuttle Radar Topography Mission (SRTM) Digitial Elevation Model (DEM) was then used to compensate topographic phase, and to aid the interpretation of the interferograms (Farr et al., 2007). An adaptive filtering technique was employed to clarify the fringes and to reduce noise (Goldstein and Werner, 1998).

NHESSD
2, 4813–4830, 2014

When an interferogram stack is ready, an initial selection based on amplitude analysis determines the PS probability for individual pixels, which is followed by a phase analysis in an iterative process (Hooper, 2006). Moreover, the deformation signals of the PS pixels are isolated from the residual phase due to DEM error, atmospheric delay and noise terms. In contrast to conventional PSI techniques, StaMPS generates a time series of deformation phase from the spatially correlated nature of deformation, rather than any prior deformation models (Hooper et al., 2007; Sousa et al., 2011). In other words, StaMPS does not rely on any predefined deformation models hence has inherent advantages for monitoring non-linear deformation.

3 Tunnelling project and SAR data

The Area Of Interest (AOI) of this study is located in Düsseldorf, Germany. Düsseldorf is the seventh largest city in Germany, and lies southwest of the Ruhr urban area. More than half a million people live in this region. The altitude of Düsseldorf ranges from 30 to 160 m. In 2011, the so-called "Wehrhahnlinie" urban tunnel project in Düsseldorf was carried out (Fig. 1). A hydro-shield tunnelling process was applied, which started in April 2011 and ended in December 2011. The shield tunnelling was done by shield machine TBM (Fig. 2). The outer diameter of the tunnel is constant as 9.50 m. In this process, reinforcement steel fiber concrete and rebar were executed (Mark et al., 2012). 20 TerraSAR-X X-band images in Strip Map (SM) mode were acquired from 7 January 2011 until 31 October 2011 (Krivenko et al., 2012). The SAR data set and baseline information is shown in Fig. 3.

4 Analysis and discussions

For deformation studies, we aim to isolate the deformation signal from other components that can be considered as noise. Atmospheric error is a significant disturbance when dealing with subtle deformation signals in urban areas. Fortunately, the variation in atmospheric retardation between passes is correlated spatially and may be estimated by a low-pass filter in the spatial domain (Hooper, 2006). Similarly, estimating other terms, such as the orbital error and DEM error, is also carried out by the StaMPS approach.

The final PSI result was shown in Figs. 4 and 5. The unit of displacement is mm year^{-1} with negative values being away the satellite and positive values being towards the satellite in the line of sight. Obviously, only a small area of the western part in the velocity map lacks of PS points since it is clumpy. Nevertheless, the density of PS points is highly satisfactory when assessed as a whole.

In order to convert the deformation in LOS to the vertical direction, direction cosines in analytic geometry were applied. In other words, the direction cosines actually are the percentages of the real displacement along three directions: vertical, N–S and E–W. The actual movements are always underestimated if only LOS displacements are used. In this study, the movements were assumed as purely vertical based on a priori knowledge. As the incidence angle is around 35°, we found an underestimation of approximate 19 % of purely vertical movements when using the LOS values.

PS points are generally stable as shown, but with some interesting exceptions. As mentioned above, in this construction, compensation injections were carried out in some cases. A number of buildings on the ground along the tunnel line could benefit from compensation injections to avoid damages which would have happened due to the subsidence caused by excavation. The velocity map indicates that some points in that area have positive displacements (points with blue colour) which may be induced by such injections. A time series analysis of some points with uplift or subsidence behaviour in this area now follows.

Figure 6 shows the persistent scatterers distributing close to the start point of the excavation. For each PS point, a deformation time series was estimated from the phase values. The different components of the interferometric phase: deformation phase,

NHESSD
2, 4813–4830, 2014

DEM error, atmospheric error, orbit error and noise are described in Eq. (1) (Hooper, 2006).

$$\phi_{\text{dint}} = \phi_{\text{def}} + \phi_{\text{DEM}} + \phi_{\text{atm}} + \phi_{\text{orb}} + \phi_{\text{noise}} \quad (1)$$

The final four error terms contaminate the deformation phase. By low-pass filtering the unwrapped PS phases in time then high-pass filtering in space, StaMPS is able to estimate the spatially correlated error, which is to be subtracted. The remaining phase component will be only related to deformation while spatially uncorrelated error terms can be modelled as noise. In whole StaMPS processing, no predefined deformation model is required. Therefore, there is a possibility to derive a non-linear deformation signal. The Time series of one PS point approximate 20 m far away from the control point is plotted in Fig. 7. From January until April 2011, an impressive uplift can be seen adjacent to the start point, due to the compensation injection mentioned above. In contrast, apparent subsidence behaviour is seen later, related to the hydro-shield tunnelling process that started in April 2011. Along with the tunnelling, a levelling survey was carried out near to the start point by the State Capital of Düsseldorf. Therefore, the levelling result has been used to validate the PSI approach here, which indicates very few discrepancies (Fig. 7).

In additional, a group of points with subsidence behaviour can be found along the tunnelling line (Figs. 8 and 9), although there is no relevant report from the terrestrial observation. To confirm this, the reason of subsidence has been clarified to be a replacement of the original pavement, according to the field survey.

5 Conclusions

An evaluation of InSAR to process-related monitoring was presented in this paper. A total of 19 interferograms were formed from 20 TerraSAR-X scenes and processed by the PSI method integrated in StaMPS, in order to monitor the deformation of the ground surface induced by a tunnelling project in Düsseldorf city in 2011. The comparison

NHESSD
2, 4813–4830, 2014

between the time series retrieved from PSI and from the leveling from a control point indicated good consistency. It is therefore concluded that InSAR/StaMPS is able to detect subtle movements for process-related monitoring in urban area with an 11 day data sampling rate, by restraining various error resources.

Acknowledgements. TerraSAR-X images were provided by DLR (CAL 1140). The levelling survey was provided by the State Capital of Düsseldorf.

References

Bamler, R. and Hartl, P.: Synthetic aperture radar interferometry, Inverse Probl., 14, R1, doi:10.1088/0266-5611/14/4/001, 1998.

Berardino, P., Fornaro, G., Lanari, R., and Sansosti, E.: A new algorithm for surface deformation monitoring based on small baseline differential SAR interferograms, IEEE T. Geosci. Remote, 40, 2375–2383, 2002.

Catalao, J., Nico, G., and Conde, V.: Detection of Ground Subsidence in the City of Lisbon: Comparison of InSAR and Topographic Measurements, Urban Remote Sensing Event (JURSE), 2011 Joint, IEEE, Munich, Germany, 417–420, 2011.

Crosetto, M., Gili, J. A., Monserrat, O., Cuevas-González, M., Corominas, J., and Serral, D.: Interferometric SAR monitoring of the Vallcebre landslide (Spain) using corner reflectors, Nat. Hazards Earth Syst. Sci., 13, 923–933, doi:10.5194/nhess-13-923-2013, 2013.

Farr, T. G., Rosen, P. A., Caro, E., Crippen, R., Duren, R., Hensley, S., Kobrick, M., Paller, M., Rodriguez, E., and Roth, L.: The shuttle radar topography mission, Rev. Geophys., 45, RG2004, doi:10.1029/2005RG000183, 2007.

Goldstein, R. M. and Werner, C. L.: Radar interferogram filtering for geophysical applications, Geophys. Res. Lett., 25, 4035–4038, 1998.

Hooper, A.: Persistent scatter radar interferometry for crustal deformation studies and modeling of volcanic deformation, Stanford University, Stanford, 2006.

Hooper, A., Segall, P., and Zebker, H.: Persistent scatterer interferometric synthetic aperture radar for crustal deformation analysis, with application to Volcán Alcedo, Galápagos, J. Geophys. Res.-Sol. Ea., 112, B07407, doi:10.1029/2006JB004763, 2007.

Kampes, B. and Usai, S.: Doris: The Delft Object-Oriented Radar Interferometric Software, 2nd International Symposium on Operationalization of Remote Sensing, Enschede, the Netherlands, 20 pp., 1999.
Krivenko, A., Riedel, B., Niemeier, W., Schindler, S., Heek, P., Mark, P., and Ziem, E.: Application of Radar Interferometry for Monitoring a Subway Construction Site, Geomonitoring, Braunschweig, Germany, 2012,
Lanari, R., Lundgren, P., Manzo, M., and Casu, F.: Satellite radar interferometry time series analysis of surface deformation for Los Angeles, California, Geophys. Res. Lett., 31, L23613, doi:10.1029/2004GL021294, 2004.
Li, Z., Elliott, J. R., Feng, W., Jackson, J. A., Parsons, B. E., and Walters, R. J.: The 2010 M_w 6.8 Yushu (Qinghai, China) earthquake: constraints provided by InSAR and body wave seismology, J. Geophys. Res.-Sol. Ea., 116, B10302, doi:10.1029/2011JB008358, 2011.
Liu, D., Shao, Y., Liu, Z., Riedel, B., Sowter, A., Niemeier, W., and Bian, Z.: Evaluation of InSAR and TomoSAR for monitoring deformations caused by mining in a mountainous area with high resolution satellite-based SAR, Remote Sensing, 6, 1476–1495, 2014.
Lu, Z. and Danskin, W. R.: InSAR analysis of natural recharge to define structure of a ground-water basin, San Bernardino, California, Geophys. Res. Lett., 28, 2661–2664, 2001.
Mark, P., Niemeier, W., Schindler, S., Blome, A., Heek, P., Krivenko, A., and Ziem, E.: Radarinterferometrie zum Setzungsmonitoring beim Tunnelbau, Bautechnik, 89, 764–776, 2012.
Massonnet, D., Rossi, M., Carmona, C., Adragna, F., Peltzer, G., Feigl, K., and Rabaute, T.: The displacement field of the Landers earthquake mapped by radar interferometry, Nature, 364, 138–142, 1993.
Osmanoğlu, B., Dixon, T. H., Wdowinski, S., Cabral-Cano, E., and Jiang, Y.: Mexico City subsidence observed with persistent scatterer InSAR, Int. J. Appl. Earth Obs., 13, 1–12, 2011.
Pritchard, M. and Fielding, E.: A study of the 2006 and 2007 earthquake sequence of Pisco, Peru, with InSAR and teleseismic data, Geophys. Res. Lett., 35, L09308, doi:10.1029/2008GL033374, 2008.
Schindler, S., Hegemann, F., Alsahly, A., Barciaga, T., Galli, M., Lehner, K., and Koch, C.: An interaction platform for mechanized tunnelling. Application on the Wehrhahn-Line in Düsseldorf (Germany)/Eine Interaktionsplattform für maschinelle Tunnelvortriebe, Anwendung am Beispiel der Wehrhahn-Linie in Düsseldorf, Geomech. Tunnel., 7, 72–86, 2014.

NHESSD
2, 4813–4830, 2014

Process-related deformation monitoring by PSI using HR space-based SAR data

D. Liu et al.

Sousa, J. J., Hooper, A. J., Hanssen, R. F., Bastos, L. C., and Ruiz, A. M.: Persistent scatterer InSAR: a comparison of methodologies based on a model of temporal deformation vs. spatial correlation selection criteria, Remote Sens. Environ., 115, 2652–2663, 2011.
Sowter, A.: Orthorectification and interpretation of differential InSAR data over mountainous areas: a case study of the May 2008 Wenchuan Earthquake, Int. J. Remote Sens., 31, 3435–3448, 2010.
Sowter, A., Bateson, L., Strange, P., Ambrose, K., and Syafiudin, M. F.: DInSAR estimation of land motion using intermittent coherence with application to the South Derbyshire and Leicestershire coalfields, Remote Sens. Lett., 4, 979–987, 2013.

NHESSD
2, 4813–4830, 2014
Process-related deformation monitoring by PSI using HR space-based SAR data
D. Liu et al.

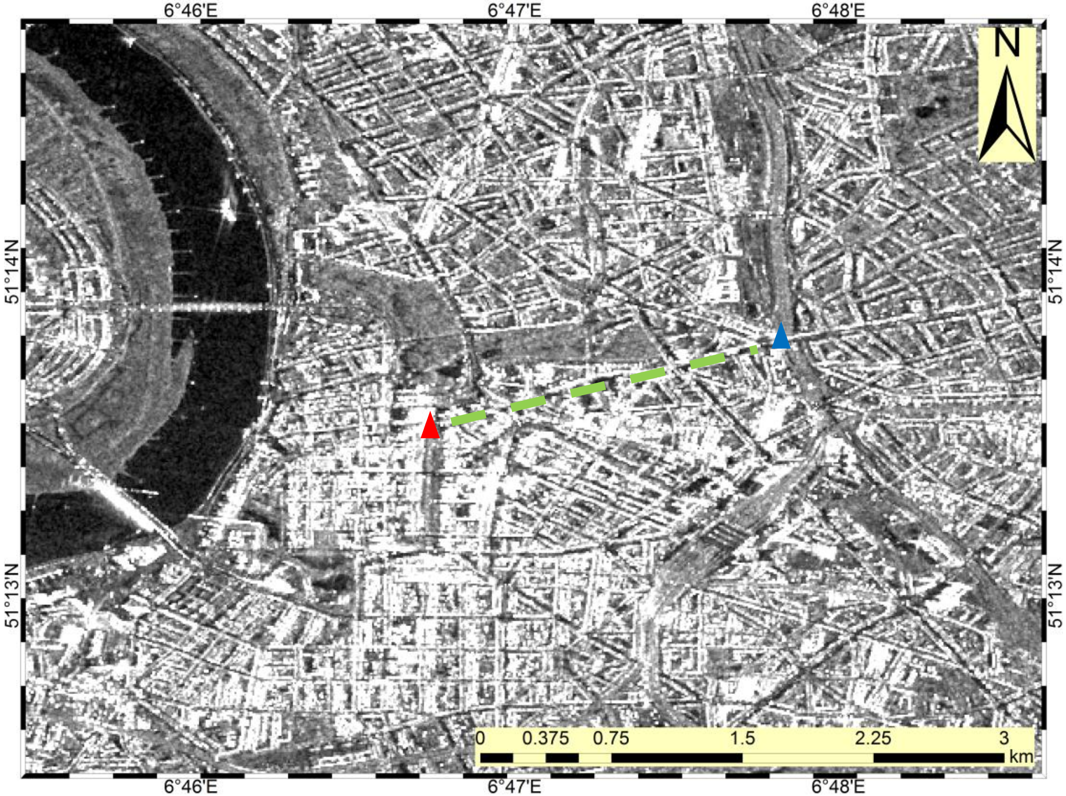

Figure 1. Approximate location of subway line construction shown on radar image by a green dotted line. Red triangle is the start point when blue triangle is the end point of the excavation.

Figure 2. Shield machine TBM arriving in the target shaft (Mark et al., 2012).

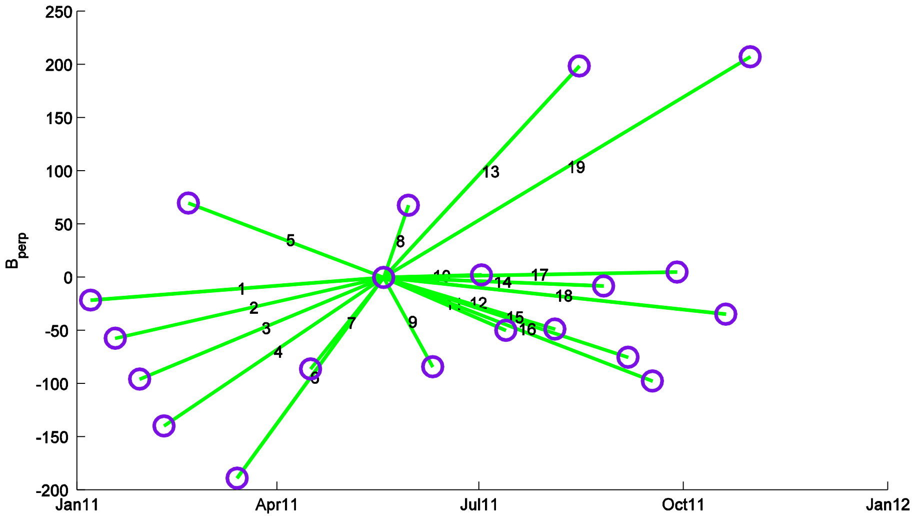

Figure 3. Interferogram pairs of TerraSAR data used. B_{perp} means the perpendicular baseline. Blue circles indicate satellite positions, when green lines indicate baselines.

NHESSD

2, 4813–4830, 2014

Process-related deformation monitoring by PSI using HR space-based SAR data

D. Liu et al.

Title Page
Abstract
Introduction
Conclusions
References
Tables
Figures
◀❙ ❙▶
◀ ▶
Back
Close
Full Screen / Esc
Printer-friendly Version
Interactive Discussion

Figure 4. Velocity map of PS points in Düsseldorf city centre, displayed on Google Earth.

NHESSD
2, 4813–4830, 2014

Process-related deformation monitoring by PSI using HR space-based SAR data

D. Liu et al.

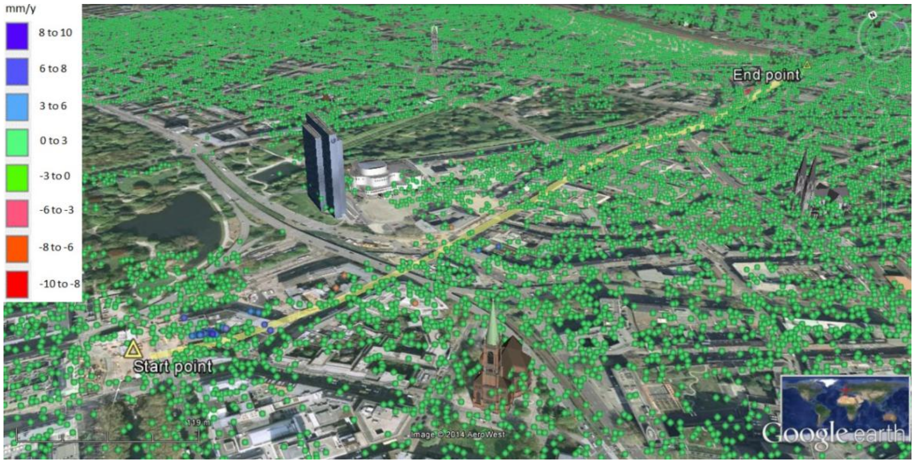

Figure 5. 3-D view of velocity map, displayed on Google Earth. The yellow line indicates the approximate location of tunnelling.

NHESSD
2, 4813–4830, 2014

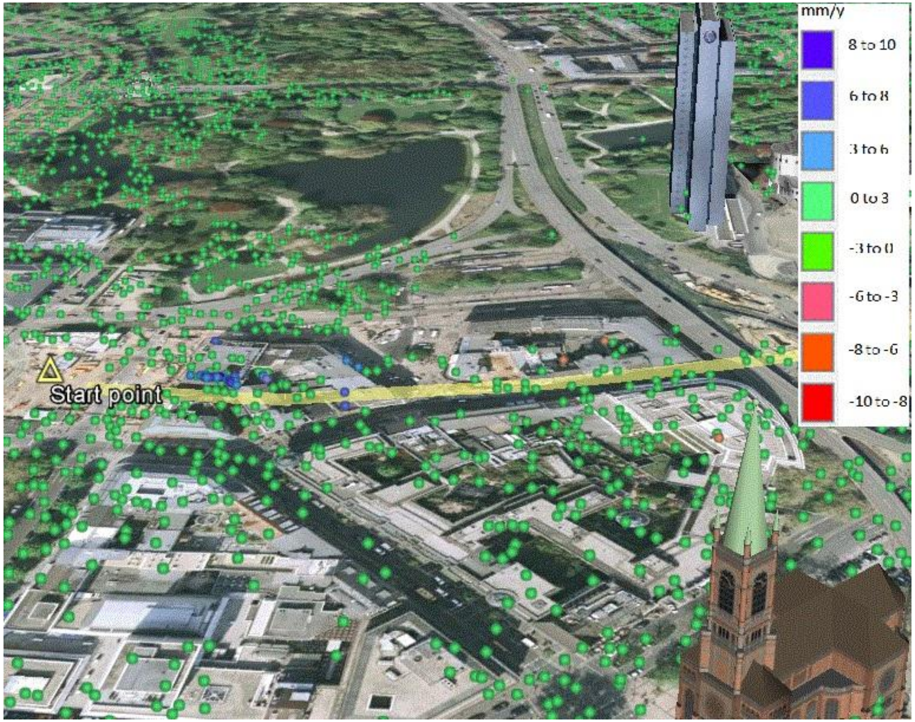

Figure 6. PS points close to the start point of the tunnelling excavation, displayed on Google Earth. The yellow line indicates the approximate location of the tunnelling line.

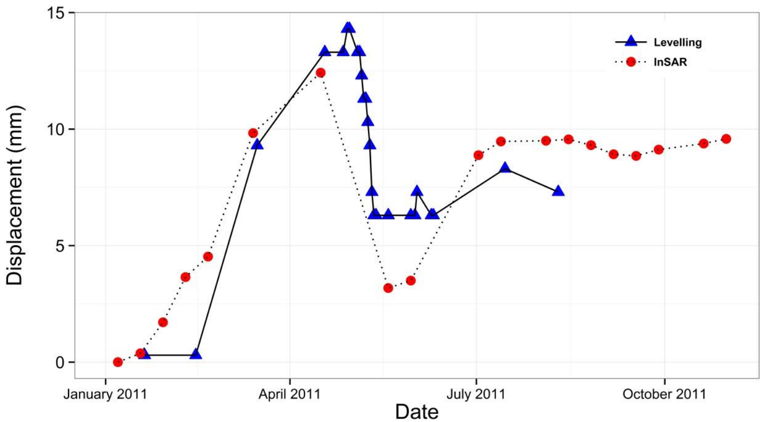

Figure 7. Comparison of deformation time series observed by levelling and PSI at the control point.

Figure 8. PS points close to the end point of the tunnelling excavation, displayed on Google Earth. The yellow line indicates the approximate location of the tunnelling line.

NHESSD
2, 4813–4830, 2014

Process-related deformation monitoring by PSI using HR space-based SAR data

D. Liu et al.

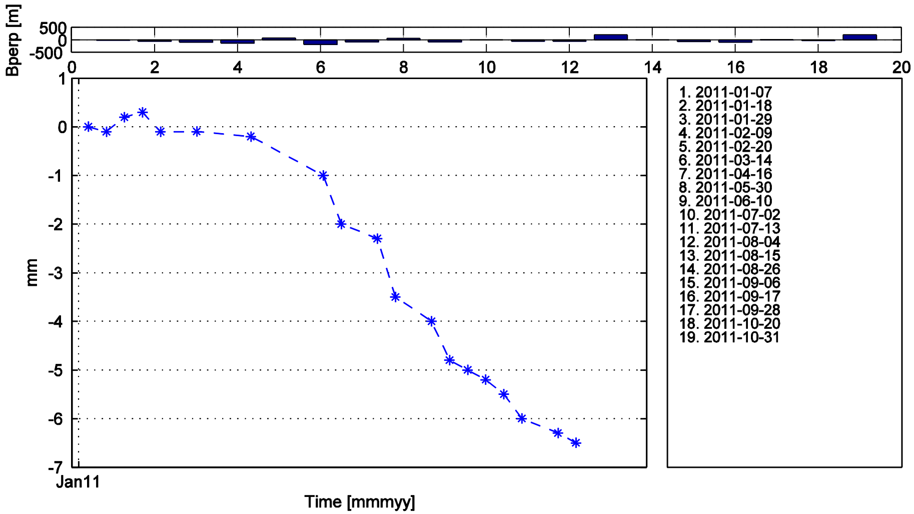

Figure 9. Deformation time series of one selected PS point near to the end point of tunnelling. B_{perp} is the perpendicular baseline of SAR pairs.

NHESSD
2, 4813–4830, 2014

Process-related deformation monitoring by PSI using HR space-based SAR data

D. Liu et al.

Title Page
Abstract Introduction
Conclusions References
Tables Figures
◀I ▶I
◀ ▶
Back Close
Full Screen / Esc
Printer-friendly Version
Interactive Discussion